Carbohydrate Research, 229 (1992) 195–211
Elsevier Science Publishers B.V., Amsterdam

A conformational study of α-L-Rha*p*-(1 → 2)-α-L-Rha*p*-(1 → OMe) by NMR nuclear Overhauser effect spectroscopy (NOESY) and molecular dynamics calculations

Göran Widmalm [1], R. Andrew Byrd and William Egan

Biophysics Laboratory, Center for Biologics Evaluation and Research, Food and Drug Administration, 8800 Rockville Pike, Bethesda, Maryland 20892 (USA)

(Received April 9th, 1991; accepted October 21st, 1991)

ABSTRACT

The conformational preference of the disaccharide α-L-Rha*p*-(1 → 2)-α-L-Rha*p*-(1 → OMe) (**1**) about the glycosidic torsion angles, ϕ and ψ, was studied by NMR NOESY spectroscopy and molecular mechanics calculations. The NOE data were consistent with either of two distinct conformations close to minima on a calculated ϕ/ψ potential energy surface. Starting from the lowest energy conformation, a 1-ns molecular dynamics (MD) trajectory was computed in vacuo, from which the NOE curves were simulated and compared to the experimentally observed NOESY data.

INTRODUCTION

In principle, the three-dimensional structures of carbohydrates and polysaccharides can be established by NMR nuclear Overhauser effect (NOE) spectroscopy[1,2] and molecular mechanics-based calculations[3]. In practice, however, a number of problems are encountered when using these methods. The unique deconvolution of NOE data in terms of structure in non-rigid molecules is often not possible because of the large number of parameters that are involved in the data fitting (internuclear distances and populations for each conformer), especially if the overall rotational diffusion of the carbohydrate is anisotropic. Problems with molecular mechanics-based calculations stem from the lack of proven, general parameter sets and, for molecular dynamics (MD) simulations, difficulties in calculating trajectories over the NOE time scale, especially if solvent (water) is included. These difficulties increase with increasing size of the molecular system. We now report efforts to obtain structural parameters for the relatively simple

Correspondence to: Dr. W. Egan, Biophysics Laboratory, Center for Biologics Evaluation and Research, Food and Drug Administration, 8800 Rockville Pike, Bethesda, MD 20892, USA.
[1] Present address: Department of Organic Chemistry, Arrhenius Laboratory, Stockholm University, S-106 91 Stockholm, Sweden.

disaccharide α-L-Rha*p*-(1 → 2)-α-L-Rha*p*-(1 → OMe) (**1**) based on NOESY and molecular mechanics studies.

EXPERIMENTAL

Disaccharide nomenclature conventions.—Atoms in the glycosyl group are assigned primed numbers; those in the methyl glycoside are unprimed. The glycosidic torsion angle ϕ is defined by the atoms O-5′–C-1′–O-2–C-2 and ψ by the atoms C-1′–O-2–C-2–C-1; the torsion angles are 0° for the *cis* conformations and, when viewed along the central bond, a clockwise rotation of the far bond is defined as positive.

General.—NMR solvents (D_2O and Me_2SO-d_6; Aldrich Chemical Co.) were of the highest isotopic enrichment available.

NMR spectra were recorded with a JEOL GSX 500-MHz NMR spectrometer. Carbon-13 relaxation times were determined using a standard inversion–recovery $(180–\tau–90)_n$ pulse sequence[4]. The determination of ^{13}C T_1 values at +37 and −30° used 6 τ-values, a 12-μs 90° pulse, and an 8.0-s delay between each 180–τ–90 pulse cycle; 800 and 2000 free induction decay (FID) signals were averaged for each τ-value at 37 and −30°, respectively; ^1H decoupling was used throughout.

NOESY spectroscopy; data acquisition and processing.—Following exchange of the hydroxyl protons for deuterons, the disaccharide was dissolved in 0.5 mL of D_2O to constitute a 40 mM solution. Ethylenediamine tetra-acetic acid (disodium salt; 0.1 mM) was added to help minimize the effects of adventitious paramagnetic ions. Oxygen was removed from the sample by repeated freeze–thaw cycles; following the final freeze–thaw cycle, the sample was vented to high-purity argon and sealed. For the low temperature measurements, a solvent mixture of D_2O (0.7 mole fraction) and Me_2SO-d_6 (0.3 mole fraction) was used[5].

A sweep width of 2500 Hz and 90° pulse width of 9.0 μs were used. Each phase-sensitive NOESY data set, consisting of spectra at differing mixing times, was collected without removing the sample from the spectrometer or altering gain or frequency settings; samples were run non-spinning to reduce t_1 noise. Phase-sensitive hyper-complex NOESY data[6] were collected so as to eliminate all first-order phase corrections and their associated baseline distortions[7]. The normal three-pulse NOESY sequence was extended with a Hahn-echo[8] in the t_2 dimension to provide accurate intensities of the first few data points and flat baselines without first-order phase corrections; the use of the echo did not alter the values of the measured NOE enhancements. In the t_1 dimension, data were sampled in a fashion that accounted for finite delays by omitting the normal initial value of t_1 (typically 5 μs plus the duration of the pulses); instead, the first data point was sampled at $t_1 = \Delta t_1 - (4 \times \tau_{90}/\pi)$, wherein Δt_1 is the dwell time for each acquired data point. The first data point in t_1 was calculated during data processing via a linear prediction scheme[9]. The *J*-cross-peaks were suppressed by variation of the

mixing time (by 5% or 15 ms for 300 ms or longer)[10]. In the t_2 domain, 1024 complex points were collected; 256 points were collected in the t_1 domain. For each t_1 value, 2×16 scans were collected with a relaxation delay > 4.0 s between transients.

The 2D data set was transferred to a MicroVax II computer and processed with the FT NMR software package (Hare Research, Inc.). A 90°-shifted sine-bell function, followed by apodization with a broadening factor of 2 Hz, was applied in the t_2 dimension. Spectra were phased manually into the pure absorption mode. In the t_1 dimension, a linear prediction algorithm was applied to the initial 30 data points to back-calculate the first point, $t = 0$. Data sets in the t_1 dimension were zero-filled ($1 \times$), and a 90°-shifted sine-bell function, which decreased to zero at the 256th data point with a 4-Hz broadening factor, was applied prior to Fourier transformation. Polynomial baseline corrections were used in both dimensions to correct residual base line anomalies. Integration of peak volumes was accomplished in the FT NMR software with an elliptical base. The intensities of autopeaks throughout the NOE build-up curve were referenced to the value of the autopeak extrapolated to a zero mixing time.

The analysis of NOE build-up curves was based on eq *1* (see below). Computer programs to generate NOE trajectories for a given input geometry were written in FORTRAN 77; all computations were carried out using double-precision arithmetic. Algorithms presented in *Numerical Recipes*[11] for obtaining the eigenvalues and eigenvectors of a real, symmetric matrix (Householder and QL algorithms) were modified for use in the above programs.

Molecular mechanics computational procedures.—The molecular mechanics program, CHARMM[12], was used for the theoretical calculations. The carbohydrate parameter set of Ha et al.[13], together with Polygen's all hydrogen set PARAM20, were used for the potential energy functions. The partial atomic charge of the glycosidic oxygen was set to -0.40 and the charges of the carbons involved in the glycosidic linkage were reduced by 0.05 unit.

The disaccharide was built from the $^1C_4$ conformation of α-L-rhamnopyranose. The ϕ/ψ map was produced from a 10° grid search over the entire glycosidic torsion-angle space using a dielectric constant of 1. At each grid point, constrained minimizations by 50 steps of steepest descent were followed by an adopted basis Newton–Raphson minimization[12] until the rms gradient was less than 0.01 kcal/(mol · Å). Four energy minima on the potential energy surface were identified in this manner. Starting at grid points close to each of the potential energy minima, unconstrained minimizations were performed to give the ϕ/ψ angles and relative energies associated with these minima.

Molecular dynamics (MD) simulations were carried out using the Verlet algorithm[14] with a time-step of 0.5 fs. A shifting function with a 22 Å cut-off was applied for long-range truncation of the interatomic non-bonded interactions[12].

The in vacuo dynamics trajectory was started from the lowest energy conformation found in the potential energy map (see above). Initial velocities were chosen

from a Boltzmann distribution at 100 K and were scaled every 100 fs by a factor proportional to an increase of 5 K until 310 K was obtained. The time for heating and equilibrium was 50 ps. Trajectory frames were saved every 0.5 ps.

The ϕ/ψ map was calculated on an Apollo DN 10000 computer; the molecular dynamics simulations were carried out on a host Apollo DN-590 or DSP-90 computer attached to a Star Technologies ST-50 array processor.

RESULTS AND DISCUSSION

For a *rigid* molecule undergoing *isotropic* rotational reorientation, and neglecting complexities due to strong scalar coupling[15] and cross-correlation effects[16], the cross-peak intensity between proton pairs in NOESY spectrum for a given mixing time, τ_m, is a function of the distance between the protons (r_{ij}), the overall rotational correlation time of the molecule (τ_c), and the ^{1}H-NMR resonance frequency (ω)[1,2,17]. The intensity of the NOESY cross-peak can be readily calculated in a manner which includes the effects of all nuclear spins, i.e., includes "spin-diffusion". For any mixing time, τ_m, the intensity of the cross-peak between nuclei i and j is the value of the i,jth element of the matrix Γ (eq *1*). The diagonal elements of Γ are the normalized autopeak intensities (having unit intensity at zero mixing time).

$$\Gamma(\tau_m) = \chi \exp(-\Lambda\tau_m)\chi^{-1} \qquad (1)$$

In eq *1*, χ is the column matrix of eigenvectors, χ^{-1} is the inverse of χ, and Λ is the diagonal matrix of eigenvalues associated with the relaxation matrix, **R**, whose elements are defined as eq *2*. The diagonal (R_{ii}) and off-diagonal (R_{ij}) elements of **R** are given as:

$$R_{ii} = \sum_{i \neq j}[2W_1(ij) + W_0(ij) + W_2(ij)] + R_{ex}(i) \qquad (2a)$$

$$R_{ij} = W_2(ij) - W_0(ij), \qquad (2b)$$

where,

$$W_1(ij) = (3/20)(r_{ij})^{-6}\alpha[\tau_c/(1+\omega^2\tau_c^2)],$$

$$W_2(ij) = (12/20)(r_{ij})^{-6}\alpha[\tau_c/(1+4\omega^2\tau_c^2)],$$

$$W_0(ij) = (2/20)(r_{ij})^{-6}\alpha\tau_C,$$

$$\alpha = \gamma^4\hbar,$$

$\hbar$ is Planck's constant divided by 2π, and γ is the proton magnetogyric ratio. $R_{ex}(i)$ represents, in an ad hoc manner, contributions to the spin-lattice relaxation of spin "i" from external sources, such as dissolved oxygen or paramagnetic metal ions[2,17]. Cast into matrix form, $\Gamma(t)$ represents the solution,

$$\mathbf{M}(t) = \Gamma(t)\mathbf{M}_0,$$

to the system of differential equations, first presented by Solomon[18] for two spins,

$$\frac{d\mathbf{M}}{dt} = -\mathbf{R}\mathbf{M}_0,$$

where **R** is as in eq *2*, **M** is a column matrix of values for the instantaneous magnetizations of the spins in the system, and $\mathbf{M}_0$ is the column matrix of initial values for the magnetization of the spins in the system. Macura and Ernst[19] have discussed the two-spin NOESY experiment in detail. Solomon's equations have been generalized[1] to the *n*-spin case (cf. ref. 16). Equation *1* can be expressed equivalently as[20]:

$$\Gamma(\tau_m) = \exp(-\mathbf{R}\tau_m), \quad (3)$$

and expanded in a Taylor series[20],

$$\Gamma(\tau_m) = \mathbf{I} - \mathbf{R}\tau_m + (\mathbf{R}\tau_m)^2/2 - (\mathbf{R}\tau_m)^3/6 + \ldots \quad (4)$$

In eq *4*, **I** is the identity matrix. For short mixing times, i.e., when $(\mathbf{R}\tau_m)^2/2$ and higher order terms are negligible relative to $\mathbf{R}\tau_m$, the NOE cross-peak intensity is equal to $R_{ij}\tau_m$.

Each off-diagonal element of **R** is a function of τ_c, r_{ij}, and the resonance frequency. In order to determine distances from cross-peak intensities, τ_c must be known. For this purpose, provided that the cross-peak intensity build-up is in the linear regime, the cross-peak intensity between a proton pair having a known, fixed distance can be used. Thus, an unknown distance, r_{ij}, can be calculated[17] from eq *5*,

$$r_{ij} = r_{ref}\left[\mathrm{NOE}_{ref}/\mathrm{NOE}_{ij}\right]^{1/6} \quad (5)$$

where r_{ref} and NOE_{ref} correspond to the internuclear distance and cross-peak intensity of the known proton pair while NOE_{ij} is the cross-peak intensity between the spins *i* and *j* whose distance is being determined. Alternatively, the correlation time can be estimated from, for example, ^{13}C or ^{2}H relaxation-time measurements, and distances calculated directly from the NOE cross-peak intensity ($R_{ij} \times \tau_m$); however, when additional relaxation mechanisms are present but are not included in the analysis, the use of correlation times obtained from ^{13}C or ^{2}H relaxation time studies can be problematic.

Estimates of R_{ij} may also be obtained experimentally by fitting NOESY data to eq *4* to second order. Thus, the values of NOE cross-peak intensities divided by τ_m can be plotted as a function of τ_m and fit by the method of least-squares to the equation of a straight line; the intercept of this line with the axis of ordinates provides an estimate of R_{ij}.

NOE build-up curves were obtained[5] for solutions of **1** in D_2O and D_2O–Me_2SO-d_6 at 37° and D_2O–Me_2SO-d_6 at −30°. All *direct* NOE's at 37° were positive (on the opposite side of the 2D plane as the autopeaks), a consequence of $\omega\tau_c$ being > 1; at −30°, all observed NOE's were negative, a consequence of $\omega\tau_c$ being < 1. The NOE's became vanishingly small at $\sim 0°$, the temperature at which

$\omega\tau_c \approx 1.12$, and for which $W_2 - W_0 = 0$ (see eq *2a*). At 37°, NOE cross-peak intensities were weaker in absolute value and proton T_1 values were longer than these same quantities when observed at −30°.

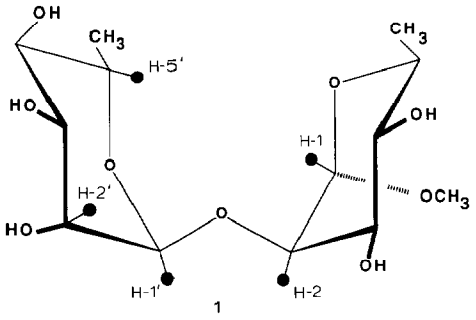

1

The long T_1 values and weak NOESY cross-peak intensities associated with **1** at 37° complicates NOE-based structural studies. First, because intensities are weak, obtaining data with good signal-to-noise ratios requires averaging a greater number of transients; this requires more spectrometer time (at 37°, the use of just 2×16 scans required ~16 h of spectrometer use per mixing time). This spectrometer time constraint is further aggravated by long T_1 values, since the spin system must return to its equilibrium state (requiring $> 5 \times T_1$) before the pulse cycle is repeated. Second, and potentially of greater significance, because the inherent proton T_1 values are long, the effects of other relaxation pathways (as from trace, adventitious paramagnetic substances) become more marked, resulting in still further reduced cross-peak intensities over much of the NOE trajectory*. Consequently, it is advantageous to collect NOESY data under non-extreme narrowing conditions, where the NOE is dominated by the W_0 terms (see eq *2b*), and where the NOE's are large in absolute value and have rapid build-up rates. This objective can be accomplished by lowering the sample temperature. For small molecules, such as **1**, this generally requires reducing the temperature to well below zero and for aqueous solutions, adding a co-solvent to prevent sample freezing[5].

Experimental estimates of inter- and intra-residue interproton distances (such as H-1–H-2, H-5′–H-1, and H-1′–H-2) for **1** were obtained from NOE data at 37° for a solution in D_2O by fitting the initial values of the NOE build-up curve to eq *4*, using the H-1′–H-2′ distances as a reference; see Table I. These distances were also derived from NOE data obtained at 37° for a solution in D_2O–Me_2SO and were, to within experimental error, the same; see Table I. The conformational

* As can be readily determined from eq *4*, the initial values of cross-peak intensities in a 2D NOE experiment are not diminished by traces of paramagnetic impurities or other contributors to R_{ex} since, to first order, R_{ex} occurs only on the diagonal (see eq *2a*); however, cross-peak intensity values at later times are reduced. The diagonal peaks in the 2D NOESY spectrum are, in contrast, affected by contributors to R_{ex} at all mixing times (see eq *4*).

preferences of **1** are apparently the same in the two solvent systems, or only minor conformational changes occur. Other studies[21] have addressed this issue of the conformational changes that might accompany changing the solvent from water to Me_2SO and have similarly concluded that there is no detectable conformational change, even when going from pure water to pure Me_2SO. There should be even less change on going from water to a water–Me_2SO mixture. We proceeded to analyze, in detail, the NOE data obtained at $-30°$.

A potential energy surface as a function of the ϕ and ψ angles was calculated for **1** using the molecular mechanics program, CHARMM; a portion of this map, including the three lowest energy conformations, is shown in Fig. 1. The relative energies of these minima, labelled as A, B, and C were 0.00, 0.08, and 2.65 kcal/mol, respectively; see Table II. The next-lowest energy conformation, D, had a relative energy of 5.01 kcal/mol and associated ϕ and ψ angles of $-82°$ and $-66°$, respectively; see Table II.

Experimental estimates of internuclear distances for **1** were obtained from NOESY data at $-30°$ by fitting NOE intensities to eq *4* to second order (data not shown). Assuming a fixed H-1′–H-2′ internuclear distance of 2.52 Å, and using ratios of intercepts, internuclear distances of 2.29 (2.22) and 2.46 (2.48) Å were calculated for the H-1′–H-2 and H-5′–H-1 proton pairs, respectively (the distances given in parentheses refer to values obtained from a separate NOESY experiment). These distances correspond closely to those for conformer A (see, Table II); however, to within experimental error, these distances could well be considered as consistent with conformer B. They are not in agreement with conformers C or D or other conformers having markedly different inter-residue distances. The energies of the A and B conformations were minimized using these inter-residue distances as constraints; the relevant molecular parameters for the resulting conformations, designated A′ and B′, are given in Table II.

Assuming for the moment that the conformation of **1** in solution is either A or B (or, alternatively, A′ or B′), then the NOE between the H-1 and H-1′ protons might be used to experimentally distinguish between them (see Table II). From the H-1–H-1′ cross-peak intensities at short mixing times (< 100 ms), an H-1–H-1′

TABLE I

NOE-based internuclear distances (Å) for **1** determined under different solvent/temperature conditions [a]

Proton pair	D_2O (37°)	D_2O–Me_2SO (37°)	D_2O–Me_2SO (−30°)
H-1–H-2	2.63	2.59	2.59
H-5′–H-1	2.50	2.47	2.46
H-1′–H-2	2.26	2.34	2.29
H-1′–H-1	–	–	3.35

[a] Distances were determined by fitting the NOE data to eq *4* to second order. The H-1′–H-2′ proton pair was used as a reference distance and was set to 2.52 Å.

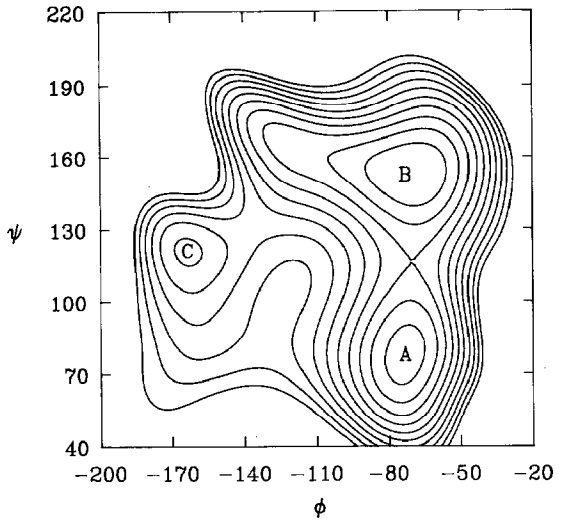

Fig. 1. A contour plot of the conformational energy of **1** as a function of the ϕ and ψ angles computed by restraining the ϕ, ψ torsional angles and minimizing the energy, as detailed in the Experimental Section. The dielectric constant used with the CHARMM potential was set to 1. Contours are drawn at 0.5 kcal/mol increments and are relative to the global minimum, which was set to 0.0 kcal/mol.

distance of 3.35 Å was calculated. This distance is consistent only with conformer A (or A′).

Based on the above data, **1** is most simply described as having a single conformation, namely, A (or A′). Moreover, this result is consistent with that of previous studies[22], wherein it was shown that the potential energy surface for an α-(1 → 2)-linked mannosyl disaccharide possessed a single, deep minimum with ϕ/ψ values of $\sim -60/0$[22a] $(-60/-20)$[22b]. When adjusted for differences in dihedral angle conventions and saccharide chirality (D-mannose vs. L-rhamnose), the ϕ-angles found for the mannosyl and rhamnosyl disaccharides are nearly equal and the ψ-angles for the mannosyl disaccharide are between the A and B minima

TABLE II

Selected internuclear distances and ϕ, ψ angles for energy-minimized conformers of α-L-Rha*p*-(1 → 2)-α-L-Rha*p*-(1 → OMe)

Conformer	Energy (kcal/mol)	ϕ (deg)	ψ (deg)	H-1′–H-2 (Å)	H-5′–H-1 (Å)	H-1′–H-1 (Å)
A	0.0	−72	80	2.32	2.63	3.24
B	0.1	−72	151	2.58	2.76	4.43
C	2.6	−163	121	2.32	4.72	3.16
D	5.0	−82	−66	3.69	5.08	2.86
A′	0.1	−71	84	2.26	2.48	3.31
B′	0.9	−76	136	2.26	2.48	4.17

[a] The A′ and B′ conformers were minimized using NOE distance constraints for H-1′–H-2 and H-5′–H-1 distances.

found herein for **1**. However, a more demanding analysis of the NOESY spectra for **1** reveals a problem with concluding that **1** is rigid and in an A-type conformation. Additionally, more realistic molecular mechanics simulations indicate that **1** is fairly flexible and, simultaneously, through comparison of the MD simulations with the experimental NOESY data, point to a possible problem with the MD potential functions.

Full NOESY trajectories were calculated for **1** in order to assess the degree to which the A′ and B′ conformers fit the entire NOESY build-up curve as well as to evaluate the sensitivity of the NOESY data to structural variations. A value for the rotational correlation time for **1** is required in order to calculate the NOESY data. This value was estimated by observing the agreement between experimental and calculated autopeak intensities for both A′ and B′ geometries using estimated values of τ_c. Since the autopeak decay rate is a function of sums of internuclear distances (eq *2a*), it is generally fairly insensitive to exact geometry; however, the autopeak decay rate is sensitive to correlation time. The calculated decay of the H-1′ autopeak for three values of the correlation time is shown in Fig. 2, along with the experimentally observed values. The best agreement between experimental and theoretical autopeak intensities occurred using a correlation time of ~ 10 ns. This method appears to be able to distinguish a factor of two difference in τ_c. A ^{13}C-NMR relaxation time measurement of **1** at $-30°$ (data not shown) furnished an independent evaluation of the correlation time. Carbon-13 T_1 values were found to be in the range 700–800 ms, depending on the carbon atom. For an isotropically reorienting C–H vector of length 1.09 Å (at 125 MHz), this corresponds to correlation times between ~ 8 and 9 ns or between 0.06 and 0.07 ns, depending on whether the molecule is in the non-extreme or extreme narrowing regime, respectively. It is highly unlikely that **1** is in the extreme narrowing regime at $-30°$. However, to prove this point, carbon relaxation times were measured at a higher temperature, $\sim 0°$; the measured T_1 values at 0° were significantly shorter (~ 300 ms) than those at $-37°$, demonstrating that **1** must be in the non-extreme narrowing regime at $-30°$. Moreover, the measured relaxation times and derived rotational correlation times are consistent with those published by Kovacs et al.[5] for a set of disaccharides in a D_2O–Me_2SO solvent mixture at various temperatures. The small range of T_1 values found for the different carbon atoms indicate that **1** is tumbling isotropically, or nearly so.

Theoretical curves for the H-1′–H-2′ and H-1–H-2 cross-peak trajectories for the A′ and B′ conformations of **1**, as well as the experimentally determined cross-peak intensities at various mixing times, are shown in Fig. 3A. The theoretical curves are in good agreement with the experimental data throughout the trajectory; that is, to within the experimental error, the data points lie on or near the computed trajectory. Since the H-1′–H-2′ and H-1–H-2 distances are known, this agreement is primarily an indicator of the accuracy of the estimated correlation time. The NOE's do not directly shed much light on the solution conformation of **1**, although they do rule out, inter alia, conformations having relatively short

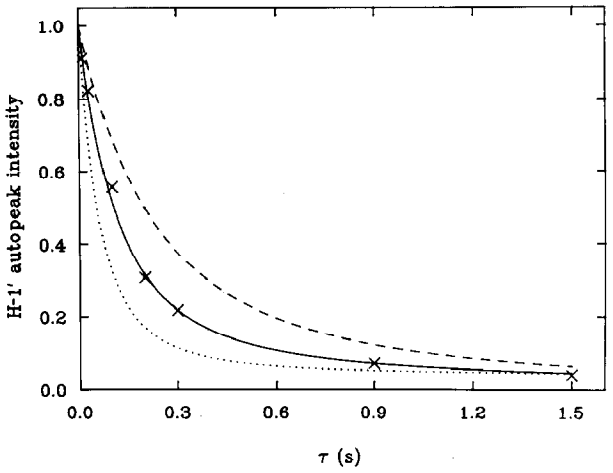

Fig. 2. Plot of the calculated H-1′ autopeak intensity (based on eq *1*) as a function of mixing time for different values of the rotational correlation time, τ_c; ———, 10 ns; - - - - - -, 5 ns; · · · · · ·, 20 ns. The experimental values at the different mixing times are indicated as ×'s. The solid curve (10 ns) is the superposition of the individual curves calculated using the A′ and B′ geometries of **1**; the other two curves represent the A′ geometry, but there was no marked difference in the autopeak decay curves generated for the B′ conformer.

H-1–H-1′ distances, as this eventuality would cause the cross-peak intensity to decrease more rapidly.

Theoretical H-1′–H-2 NOE trajectories for the A′ and B′ conformers of **1** are shown in Fig. 3B along with the experimentally measured values for different mixing times. Since the H-1′–H-2 distance is virtually the same in these two conformations (see Table I), it is not surprising that their corresponding theoretical NOE curves are nearly identical (although indirect effects could have rendered them different at longer mixing times). The experimental values fall on the theoretical curves, demonstrating that the H-1′–H-2 distance in **1** must be approximately 2.25 Å, as it is for A′ and B′, and directly ruling out a significant population in conformations for which this distance is markedly different.

The H-5′–H-1 distances in the A′ and B′ conformers are also very similar and, again, not surprisingly, the H-5′–H-1 theoretical NOE curves for the A′ and B′ conformers are nearly the same (Fig. 3B). Except at the longer mixing times, the experimental data were in good agreement with the theoretical curves and support either A′ or B′ as the actual solution conformation of **1**. Minimally, this NOE excludes significant populations of conformers having markedly different values for this internuclear distance. The theoretical curves were generated using average internuclear distances between the methyl group protons and the other sugar-ring protons, namely, $\langle r_{ij}^3 \rangle^2$, where $\langle \ldots \rangle$ indicates an average (see below). As noted, the H-5′–H-1 NOE data fit well at the shorter mixing times, where the direct NOE effects dominate. The decay of the NOE trajectory at the longer mixing times is due, in part, to a transfer of magnetization from H-5′ to the C-6′ methyl protons;

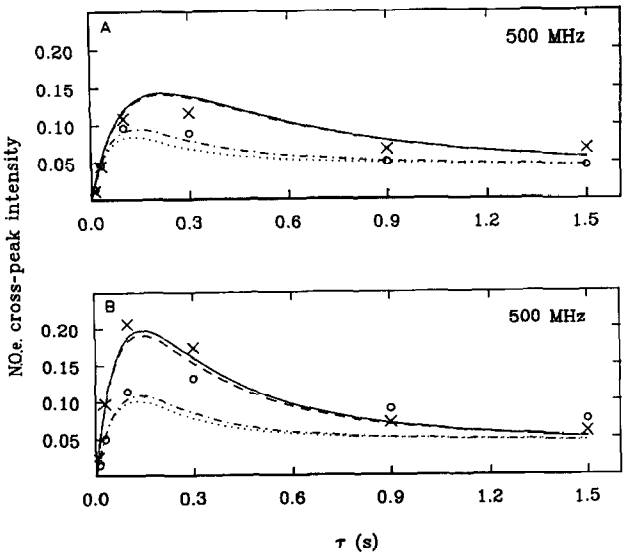

Fig. 3. A, Theoretical and experimental ^{1}H NOESY (500 MHz) cross-peak intensities for different proton pairs as a function of mixing time, using a 10-ns value for τ_c. The solid- and dashed-line trajectories refer to H-1′–H-2′ for the A′ and B′ conformers, respectively; the corresponding experimental points for the various mixing time are indicated as ×'s. The alternating dash-dot- and the dotted-line trajectories refer to H-1–H-2 for the B′ and A′ conformers, respectively; the corresponding experimental points are indicated in the curve as ○'s. The theoretical trajectories were calculated from equation *1* as described in the Experimental Section. B, Theoretical and experimental ^{1}H NOESY (500 MHz) cross-peak intensities for proton pairs as a function of mixing time, using a 10-ns value for τ_c. The solid and dashed trajectories refer to the theoretical H-1′—H-2 cross-peak intensities for the A′ and B′ geometries, respectively. The experimental points are represented as ×'s. The dash-dot and dotted lines refer to the theoretical trajectories for the H-5′–H-1 NOE for the B′ and A′ conformations, respectively; the experimental values at the different mixing times are presented as ○'s.

the effective correlation time for this interaction is likely to be different (and shorter) from that for the other internuclear vectors. However, we have not tried to adjust the correlation time for the methyl to sugar-ring proton interactions to better fit the NOE data since there would be no simple way to assess independently its correctness. Furthermore, it is likely that cross-correlation effects[16] could also alter the NOE behavior of protons interacting with the methyl group at these longer mixing times.

The low-temperature NOE data support a disaccharide conformation having inter-residue distances that are consistent with either A′ or B′ conformations of **1**. This point is readily visualized, and extended, in Fig. 4, wherein the loci of ϕ/ψ values having fixed H-5′–H-1 and H-1′–H-2 distances are superimposed on the potential energy surface for **1** presented in Fig. 1. The curves intercept at two regions, near the calculated A and B minima. Thus, while either internuclear distance alone is consistent with a manifold of conformational states, taken together, the number of possible states is sharply limited. Indeed, the number of possible states is limited to those in the vicinity of the A and B minima. It is, of

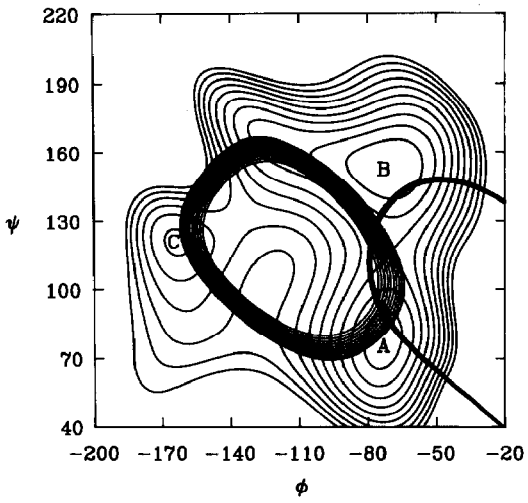

Fig. 4. Superposition of the potential energy surface presented in Fig. 1 and curves describing the loci (as ϕ/ψ angles) of points having fixed values for the internuclear distances for the indicated pairs. The H-1′—H-2 curves (complete ovals) span a set of distances from 2.2–2.3 Å in 0.01-Å increments. The H-5′—H-1 curves (partial ovals) span a set of distances from 2.45–2.50 Å, in 0.01-Å increments.

course, still possible, but unlikely, that the NOE's derive from a combination of states that have geometries that are distinctly different from A′ and B′, but that in combination fortuitously mimic them.

Since the H-1′–H-1 internuclear distances are markedly different in the A′ and B′ conformations (3.3 and 4.2 Å, respectively), the value of the NOE between them should serve to distinguish them or otherwise indicate that conformational averaging is occurring. The theoretical build-up curves for the H-1–H-1′ NOE for A′ and B′ are shown in Fig. 5A. These curves are nearly identical, even at short mixing times (50–100 ms); therefore, they cannot be used to decide if **1** adopts an A′ or B′ conformation. This surprising result, the similarity of the A and B build-up curves throughout the NOE trajectory, arises from indirect effects involving, inter alia, the H-1′–H-2 NOE. While it remains true that initial slopes can be used to derive internuclear distances, the concept of "initial slope" refers, in this particular instance, to mixing times that are exceedingly short, ~ 0.1 ms or less; the cross-peak intensities for the A′ and B′ conformers at these mixing times are, in any practical sense, impossible to measure experimentally. It is also apparent that the use of the complete NOESY trajectory cannot distinguish A′ from B′. The importance of indirect effects is demonstrated in Fig. 5B, wherein the H-1–H-1′ NOE curves for the A′ and B′ conformations are plotted for the disaccharide in which H-2, or its effect, is deleted, as, for example, by deuteration or the use of MINSY[23] or SLOESY[24] NMR sequences.

A molecular dynamics trajectory has been calculated for **1** in vacuo at −30°. This trajectory was initiated from the A conformation and extended to 1 ns. The fluctuations in ϕ/ψ angles for the trajectory are displayed in Fig. 6, along with the

associated changes in the H-1′–H-2, H-5′–H-1, and H-1′–H-1 distances. The vacuum trajectory indicates a non-rigid disaccharide; ring flips or chair-to-boat interconversions were not seen in this or other 1-ns trajectories that were run using different values of the dielectric constant or with included solvent (data not shown). From Fig. 6, it can be seen that **1** is in the A conformation for the majority of the trajectory. A transition from the A to B conformation is seen at ~460 ps into the trajectory, with the molecule remaining in the B conformation until ~690 ps, thereafter returning to the A conformation. Near the end of the trajectory, a transition from the A to the C conformation is observed; however, the molecule is seen to spend only ~15 ps in the C conformation before returning to the A conformation. Considered as the simplest three-state system, and using the relative energies found in Table I, the equilibrium fractional populations for the A, B, and C conformers predicted by the Boltzmann distribution equation are 0.5504, 0.4471, and 0.0025, respectively. The relative residence times of **1** in the A, B, and C states (0.75, 0.23, and 0.015, respectively) derived from the MD trajectory do not match these fractional populations. This disagreement may be due to the shape of the potentials (for example, a broad vs. a narrow potential well), but may also be due to sampling errors. Even though the MD trajectory now reported is significantly longer than the majority of published saccharide trajectories (typically, 20–100 ps, but occasionally 500 ps)[3,13,22a,25], it is nonetheless far too short to obtain accurate estimations of the equilibrium populations for the A and B conformers (and certainly not the C conformer) and their associated transition rates[26]. However, the equilibrium populations could be estimated from a normal mode analysis of the potential energy map[27].

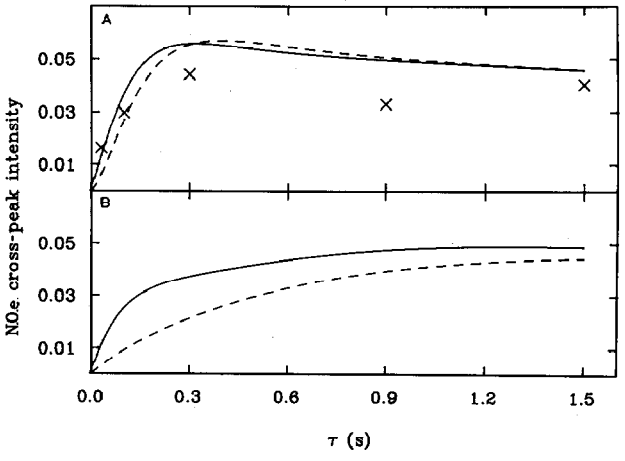

Fig. 5. A, Theoretical and experimental ^{1}H NOESY (500 MHz) cross-peak intensities for H-1′–H-1 as a function of mixing time for the A′ (solid line) and B′ (dashed line) geometries of **1**; the experimental points are indicated as ×'s. B, Theoretical ^{1}H NOESY (500 MHz) cross-peak intensities for H-1′–H-1 as a function of mixing time for **1** in which H-2 has been replaced with deuterium; the solid and dashed lines refer to the A′ and B′ geometries, respectively.

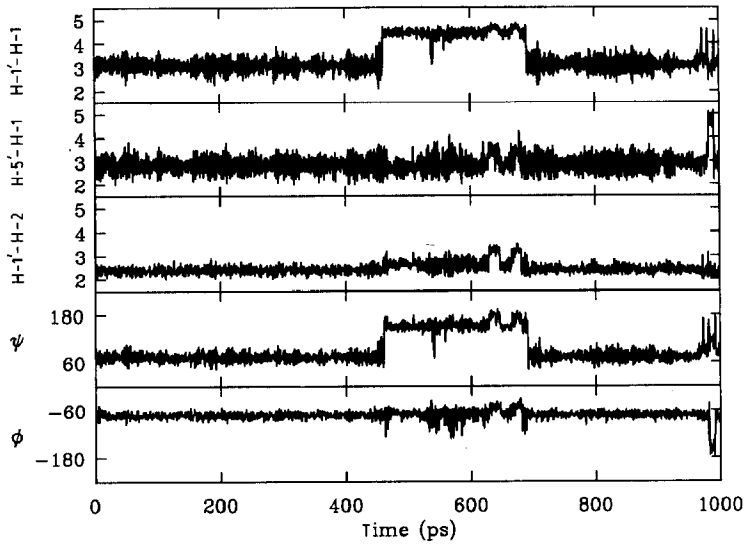

Fig. 6. History of the fluctuations of the ϕ/ψ angles and selected internuclear distances for **1**, calculated from an in vacuo MD trajectory as described in the Experimental Section. The value of the dielectric constant was set to 1.

In accord with our earlier comments, it can be seen from the trajectories presented in Fig. 6 that the H-1′–H-2 and H-5′–H-1 distances are relatively insensitive to the A/B conformational interchange, whereas the H-1′–H-1 distance is sensitive to this transition. The trajectories, however, provide additional information that is not readily apparent from the ϕ/ψ maps, namely, the amplitude of librational motions within the minima. Thus, for example, the H-5′–H-1 distance fluctuates between extreme values of 2 and 4 Å within the A and B conformations and the fluctuation of the H-1′–H-2 distance is small within the A conformation, but more extensive within the B conformation. The fluctuation of the H-1′–H-1 distance is intermediate those of H-1′–H-2 and H-5′–H-1; however, the fluctuation of the H-1′–H-1 distance is diminished in the B relative to the A conformation.

The extent to which these molecular dynamics trajectories reflect the actual behavior of the disaccharide can be evaluated by comparing theoretical NOE build-up curves, averaged over the MD trajectory, with the experimental data. Internuclear distances were averaged over the in vacuo MD trajectory in order to simulate the NOESY data. Thus, values of $\langle r^3\rangle^2$ and $\langle r^6\rangle$ were computed and substituted into eq *1* (the use of the two different averaging procedures is discussed below). Theoretical build-up curves, using the two averaging methods, are shown in Fig. 7; there is relatively little difference between NOE build-up curves based on the choice of averaging method. The overall agreement between the theoretical and experimental NOE values at differing mixing times for the intra-residue distances, H-1′–H-2′ and H-1–H-2, and the inter-residue H-1′–H-2 distance, is moderately good. However, the agreement between theoretical and

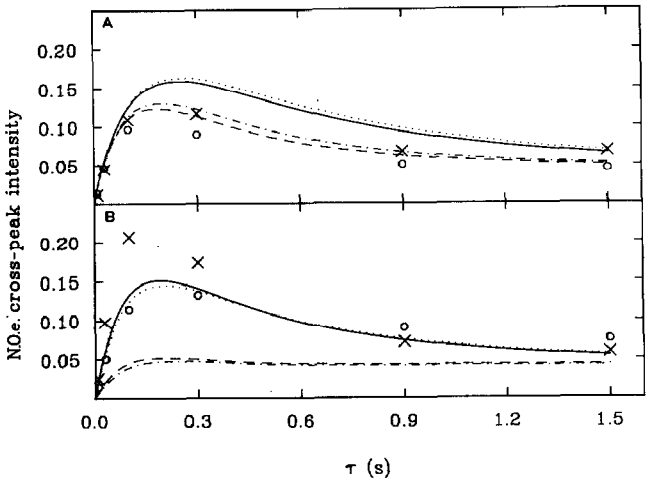

Fig. 7. Theoretical and experimental ^{1}H NOESY (500 MHz) cross-peak intensities for various proton pairs as a function of mixing time. A, The top theoretical cross-peak intensity build-up curves that were calculated for H-1′–H-2′ and H-1—H-2 by averaging over the 1-ns vacuum trajectory. The dotted and solid lines refer to the H-1′–H-2′ NOE, using $\langle r^6 \rangle$ and $\langle r^3 \rangle^2$, respectively; the dash-dot and dashed lines refer to the H-1–H-2 NOE with $\langle r^6 \rangle$ and $\langle r^3 \rangle^2$ averaging, respectively. The experimental H-1′–H-2′ and H-1–H-2 NOE's at various mixing times are indicated as ×'s and ○'s, respectively. B, The theoretical cross-peak build-up curves for the H-1′–H-2 and H-5′–H-1 NOE's calculated from the vacuum trajectory. The solid and dotted lines refer to the H-1′–H-2 NOE, using $\langle r^6 \rangle$ and $\langle r^3 \rangle^2$ averaging, respectively; the dashed and dash-dot lines refer to the H-5′–H-1 NOE's, using $\langle r^6 \rangle$ and $\langle r^3 \rangle^2$ averaging, respectively. The experimental values of the H-1′–H-2 and H-5′–H-1 NOE's are represented by ×'s and ○'s, respectively.

experimental values for the other inter-residue NOE, H-5′–H-1, is poor. From a comparison of the calculated and observed NOE enhancement, it appears that, over the MD simulation, the H-5′–H-1 distance is, on average, too long; this is particularly evidenced in the lack of agreement for the initial slope. It appears that this agreement is not the result of a dynamics trajectory that is too short, since H-5′ and H-1 are closer in the A conformation than in either the B or C conformation and it is the A conformation that may be over-emphasized in the MD trajectory.

As mentioned above, two distance-averaging schemes were used in the calculations over the dynamics trajectory. The first averaging scheme used a value of $\langle r^6 \rangle$ for computing NOE curves; this procedure is appropriate[28] when k_{inter}, the rate constant for the internal motion, is slow relative to $(\tau_c)^{-1}$. The second averaging scheme used a value of $\langle r^3 \rangle^2$; this procedure is appropriate[28] when the rate of interconversion if fast relative to $(\tau_c)^{-1}$. Additionally, when the rate of interconversion is fast relative to $(\tau_c)^{-1}$, an angular term, $(3 \cos^2 \theta - 1)$, where θ is the angle between the internuclear vector and the z-direction of the magnetic field, should be included in the determination of the spectral densities[28,29]. This additional averaging was neglected in the present calculations but, if included, would have led to theoretical build-up curves for which the nuclei would appear further

apart, thereby increasing the disparity between the calculated and observed H-5′–H-1 NOE's.

CONCLUSIONS

This study points to problems that may arise from an overly simplified analysis of NOE data; that is, an analysis based on the isolated spin-pair approximation (ISPA). Thus, while a complete treatment of the NOE data showed that *both* the A and B conformations were consistent with the experimental data, the ISPA selected the A conformer. It is still a possibility that **1** exists in solution mainly as an A-like conformer, but this remains to be proved by other experiments. Problems in interpreting NOE data, such as have been presented herein, are not limited to **1** or its analogs, but are general and emphasize the need for very thorough analyses of NOE data before drawing conclusions about the conformations of even simple carbohydrate systems.

The observation that the conformations of **1** that were consistent with the observed NOE effects correspond to the two lowest energy conformations calculated by molecular mechanics methods, using the parameters of Ha et al.[13], lends credence to these parameter sets, at least when the value of the dielectric constant was set equal to 1. The use of different values for this constant can alter the map considerably[30]. However, the overall lack of detailed agreement between observed and MD-based NOE trajectories may reflect a problem with the parameter set or arise from not explicitly including water in the calculations[22a,30]. Alternatively, as mentioned in the previous section, the lack of agreement between the MD-based and experimental NOE's may be the result of an inadequate sampling of the states. This issue will need to be addressed further. If, however, the discrepancy is due to limited sampling, then MD-based calculations may be of little use in helping to interpret NOE data in complicated systems, since it will not generally be possible to extend the trajectories to the microsecond range and alternative theoretical methods will be required.

It is certainly important to reconcile the molecular mechanics based calculations with the NOE studies of simple systems, having only a few degrees of freedom. MD simulations (or their equivalent) will be needed for the conformational analysis of biologically more relevant and more complicated oligosaccharides where it will not be possible to interpret the NOE data unambiguously in terms of conformational states and their respective populations. However, before these molecular mechanics based calculations can be used with confidence for complex systems, they must be firmly established through rigorous testing on small systems.

ACKNOWLEDGMENTS

We thank the Swedish Natural Sciences Research Council for a post-doctoral fellowship (to G.W.), Dr. M. Szoni (University of Stockholm) for the sample of **1**,

and Drs. T.E. Bull, R.W. Pastor, and R.M. Venable (Center for Biologics Evaluation and Research) for many helpful discussions.

REFERENCES

1 J.H. Noggle and R.E. Schirmer, *The Nuclear Overhauser Effect*, Academic Press, New York, 1971.
2 D. Neuhaus and M. Williamson, *The Nuclear Overhauser Effect in Structural and Conformational Analysis*, VCH Publishers, New York, 1989.
3 See, for example, A.D. French and J.W. Brady, *ACS Symp. Ser.*, 430 (1990).
4 T. Farrar and E.D. Becker, *Pulse and Fourier Transform N.M.R.*, Academic Press, New York, 1971; E.D. Becker, J.A. Ferretti, R.K. Gupta, and G.H. Weiss, *J.Magn. Reson.*, 37 (1980) 381–394.
5 H. Kovacs, S. Bagley, and J. Kowalewski, *J. Magn. Reson.*, 85 (1989) 530–541.
6 States, R.A. Haberkorn, and D.J. Reuben, *J. Magn. Reson.*, 48 (1982) 286–292.
7 E.O. Stejskal and J. Schaefer, *J. Magn. Reson.*, 14 (1974) 160–169; P. Plateau, C. Dumas, and M. Gueron, *ibid.*, 54 (1983) 46–53; D.I. Hoult, C.-N. Chen, H. Eden, and M. Eden, *ibid.*, 51 (1983) 110–117.
8 D.G. Davis, *J. Magn. Reson.*, 81 (1989) 603–607; M. Rance and R.A. Byrd, *ibid.*, 52 (1983) 221–240.
9 D. Marion and A. Bax, *J. Magn. Reson.*, 83 (1989) 205–221.
10 S. Macura, Y. Huang, D. Suter, and R.R. Ernst, *J. Magn. Reson.*, 46 (1982) 269–282.
11 W.H. Press, B.P. Flannery, S.A. Teukolsky, and W.T. Vetterling, *Numerical Recipes*, Cambridge University Press, Cambridge, 1986, pp. 335–380; see also, F.S. Acton, *Numerical Recipes that Work*, Harper & Row, New York, 1970, pp. 316–360.
12 B.R. Brooks, R.E. Bruccoleri, B.D. Olafson, D.J. States, S. Swaminathan, and M. Karplus, *J. Comput. Chem.*, 4 (1983) 187–217.
13 S.H. Ha, A. Giammona, M. Field, and J.W. Brady, *Carbohydr. Res.*, 180 (1988) 207–221.
14 L. Verlet, *Physics Rev.*, 159 (1967) 98–103; R.W. Pastor, B.R. Brooks, and A. Szabo, *Mol. Phys.*, 65 (1988) 1409–1419.
15 L.E. Kay, J.N. Scarsdale, D.R. Hare, and J.H. Prestegard, *J. Magn. Reson.*, 68 (1986) 515–525.
16 T.E. Bull, *J. Magn. Reson.*, 72 (1987) 397–413.
17 P.D. Thomas, V.L. Basus, and T.L. James, *Proc. Nat. Acad. Sci. U.S.A.*, 88 (1991) 1237–1241.
18 I. Solomon, *Phys. Rev.*, 99 (1955) 559–565.
19 S. Macura and R.R. Ernst, *Mol. Phys.*, 41 (1980) 95.
20 G. Strang, *Linear Algebra and Its Applications*, Academic Press, New York, 1976, pp. 196–229.
21 See, for example, K. Bock and R.U. Lemieux, *Carbohydr. Res.*, 100 (1982) 63–74; P. Cagas and C.A. Bush, *Biopolymers* 30 (1990) 1123–1138.
22 (*a*) C.J. Edge, U.C. Singh, R. Bazzo, G.L. Taylor, R.A. Dwek, and T.W. Rademacher, *Biochemistry* 29 (1990) 1971–1974; (*b*) T. Peters, *Liebigs Ann. Chem.*, (1991) 135–141.
23 W. Massefski and A.G. Redfield, *J. Magn. Reson.*, 78 (1988) 150–155.
24 T.E. Bull, *J. Magn. Reson.*, 93 (1991) 596–602.
25 D.A. Cumming, R.N. Shah, J.J. Krepinsky, A.A. Grey, and J.P. Carver, *Biochemistry*, 26 (1987) 6655.
26 R.W. Pastor, in V. Renugopalakrishnan, P.R. Carey, I.C.P. Smith, S.-G. Huang, and A.C. Storer (Eds.), *Proteins: Structure, Dynamics and Design*, ESCOM Science Publishers, Leiden, 1991.
27 B.M. Pettitt and M.J. Karplus, *J. Am. Chem. Soc.*, 107 (1985) 1166–1173.
28 J. Tropp, *J. Chem. Phys.*, 72 (1980) 6035–6043.
29 G. Lippari and A. Szabo, *Biochemistry*, 20 (1981) 6250–6256; D.M. LeMaster, L.E. Kay, A.T. Brunger, and J.H. Prestegard, *FEBS Lett.*, 236 (1988) 71–76.
30 W. Egan and G. Widmalm, unpublished observations.